Eur. Phys. J. B **2**, 51–56 (1998)

THE EUROPEAN PHYSICAL JOURNAL B

Surface effects in field-induced smectic transitions

P. Galatola[1,a], M. Żelazna[1,b], and I. Lelidis[2]

[1] Dipartimento di Fisica and Istituto Nazionale di Fisica della Materia, Politecnico di Torino, Corso Duca degli Abruzzi 24, 10129 Torino, Italy
[2] Département de Physique, Institut de Génie Atomique, École Polytechnique Fédérale de Lausanne, 1015 Lausanne, Switzerland

Received: 25 August 1997 / Accepted: 23 January 1998

Abstract. We study the surface behavior of a semi-infinite smectogenic sample bounded by a solid wall, in the presence of an external electric field. Our analysis is performed in the framework of a Landau-de Gennes theory. For the sake of simplicity, we consider only the case in which, in the absence of field and surfaces, a direct isotropic to smectic-A transition occurs, while in the presence of the electric field a nonspontaneous nematic phase appears. Two new surface phases are identified, namely a *parasmectic* and a *surface-induced smectic* phase. The shifts in the transition temperatures and the critical behavior of the surface states are analyzed.

PACS. 64.70.Md Transition in liquid crystals – 68.35.Md Surface energy; thermodynamics properties – 64.10.+h General theory of equations of state and phase equilibria

1 Introduction

Liquids composed of anisotropic molecules can display a rich variety of so-called mesophases [1]. The latter are intermediate states of matter between the isotropic (I) and the solid crystalline phases. The least ordered of liquid crystals is the nematic (N) one, where the molecules spontaneously align themselves with their long axes parallel. The uniaxial nematic ordering can be described by the symmetric traceless tensor $\mathbf{Q} = S(3\mathbf{n} \otimes \mathbf{n} - \mathbf{1})/2$, where $\mathbf{1}$ is the identity tensor, $\mathbf{n}$ is the nematic director, which gives the average molecular orientation, and $0 \leq S \leq 1$ is the scalar order parameter characterizing the degree of molecular orientation.

In the smectic-A (S_A) phase, molecules are additionally organized in layers perpendicular to the nematic director $\mathbf{n}$. Therefore, the density ρ is periodically modulated and can be approximated as $\rho = \rho_0[1 + (1/\sqrt{2})\psi \cos(q_s z + \phi_0)]$, where ρ_0 is the average density, $2\pi/q_s$ is the layer spacing, ϕ_0 is a reference phase, and ψ is the smectic order parameter [1].

The phase transitions between the various liquid crystalline phases usually appear while varying temperature. Another possibility is to apply external fields. In particular, when a material characterized by a positive dielectric anisotropy is subjected to an electric field, the degree of order is enhanced. In the simplest case of nematogenic substances, the appearance of a *paranematic* phase and of a critical point in the paranematic–nematic transition was predicted [2–4] and experimentally confirmed [5,6]. Even more rich behaviors emerge when smectogenic materials are considered. These were theoretically investigated in the framework of a McMillan's theory [7] and of a lattice model [8]. The existence of a nonspontaneous nematic phase and of a tricritical behavior of the nematic–smectic-A transition was predicted and observed [9]. Motivated by these experiments, a thorough analysis using a phenomenological Landau-de Gennes approach was carried out in reference [10]. All these theoretical investigations were concerned only with the bulk behavior. However, the experimental data show some unexplained features that could be attributed to surface effects [9]. More precisely, the low-field part of the nematic order-parameter isotherms displays a linear character. Additionally, a residual surface birefringence connected with smectic ordering at the surfaces was measured. These observations are in agreement with X-ray diffraction studies, that show continuous or discrete growth of smectic layers at surfaces [11, 12]. Moreover, molecular dynamics simulations indicate that smectic ordering can be favored for steric reasons close to substrates [13,14]. The effect of solid boundaries in a presmectic fluid was also analyzed by de Gennes using a Landau description [15] .

Summarizing, the combined influence of an external electric field and of limiting surfaces can induce significant changes in the thermodynamic behavior of smectogenic materials. These phenomena have not yet been analyzed, because of the complexity of the system and of the various interactions present. In this paper, by means

[a] e-mail: paolo@iris.polito.it
[b] On leave from Zakład Fizyki Statystycznej, Instytut Fizyki, Uniwersytet Jagielloński, ul. Reymonta 4, Kraków, Poland.

of a Landau-de Gennes approach, we consider a semi-infinite liquid crystalline sample bounded by a solid surface. Motivated by the experimental observations [9], we focus our attention on systems which display a direct isotropic to smectic-A phase transition in the absence of field and surfaces, with a nonspontaneous nematic phase appearing under the application of an external electric field. Following the idea of de Gennes [15], we describe the interaction of the smectogenic material with the solid substrate *via* a term linear in the smectic order parameter, assuming for the sake of simplicity that the direct interaction of the solid interface with the nematic order parameter is negligible. We compute phase diagrams in the temperature–electric field plane for various strengths of the surface coupling. The existence of parasmectic and surface-induced smectic phases is predicted. It is also shown that the bulk tricritical point is replaced at the surface by a critical one.

The paper is organized as follows: in Section 2 we present the general theoretical framework, formulating the Euler-Lagrange equations that govern the evolution of the order parameters profiles. In Section 3, solving numerically these equations, we obtain the phase diagrams describing the surface behavior of a semi-infinite smectogenic sample under the influence of an external electric field. Finally, in Section 4, we discuss our main results and the possible outlooks.

2 Landau-de Gennes theory

Let us consider a thermotropic liquid-crystalline material undergoing a direct isotropic–smectic-A transition on cooling. In the frame of a Landau-de Gennes theory of phase transitions, in the absence of elastic distortions, such a system can be described by the free-energy functional [1]

$$\mathcal{F}_{\text{bulk}} = \int \Big[f_{\text{N}}(T,S) + f_{\text{A}}(T,\psi) + f_{\text{AN}}(S,\psi) + \frac{1}{2} L_{\text{N}} \left(\nabla S\right)^2 + \frac{1}{2} L_{\text{A}} \left(\nabla \psi\right)^2 \Big] \, \mathrm{d}V \ , \tag{1}$$

where $f_{\text{N}}(T,S)$ and $f_{\text{A}}(T,S)$ are the nematic and smectic contributions, respectively, and $f_{\text{AN}}(S,\psi)$ is a coupling term

$$f_{\text{N}}(T,S) = \frac{1}{2} a_{\text{N}} (T - T_{\text{N}}^*) S^2 + \frac{1}{3} b_{\text{N}} S^3 + \frac{1}{4} c_{\text{N}} S^4 \ , \tag{2a}$$

$$f_{\text{A}}(T,\psi) = \frac{1}{2} a_{\text{A}} (T - T_{\text{A}}^*) \psi^2 + \frac{1}{4} c_{\text{A}} \psi^4 \ , \tag{2b}$$

$$f_{\text{AN}}(S,\psi) = \gamma S \psi^2 + \frac{1}{2} \lambda S^2 \psi^2 \ . \tag{2c}$$

In the latter equations T_{N}^* and T_{A}^* are the supercooling temperature limits of the isotropic and nematic phases, respectively, and T is the temperature. In order to induce a direct $\text{I} - \text{S}_{\text{A}}$ transition, a sufficiently strong coupling constant γ is required [10]. The saturation term proportional to λ allows for reentrant nematic behavior; in the following, for the sake of simplicity, we shall not analyze this case. For the Landau coefficients appearing in equations (2), we use the values given in reference [9]: $a_{\text{N}} = 0.2 \times 10^7 \,\text{erg/K}\,\text{cm}^3$, $b_{\text{N}} = -1.85 \times 10^7 \,\text{erg/cm}^3$, $c_{\text{N}} = 2.5 \times 10^7 \,\text{erg/cm}^3$, $a_{\text{A}} = 0.13 \times 10^7 \,\text{erg/K}\,\text{cm}^3$, $c_{\text{A}} = 0.25 \times 10^7 \,\text{erg/cm}^3$, $\gamma = -0.5 \times 10^7 \,\text{erg/cm}^3$, $\lambda = 0.65 \times 10^7 \,\text{erg/cm}^3$, $T_{\text{N}}^* - T_{\text{A}}^* = 0.5 \,\text{K}$. The elastic constants L_{N} and L_{A} are related to the nematic elastic constant K and to the smectic compressibility modulus B, namely $K = L_{\text{N}} S^2$, $B = L_{\text{A}} \psi^2 q_{\text{s}}^2$. Since the characteristic length $\sqrt{K/B}$ is of the order of the interlayer spacing $2\pi/q_{\text{s}}$ [1], then $L_{\text{A}}/L_{\text{N}} \sim (S/\psi)^2 \sim 1$. In our analysis we therefore set $L_{\text{A}} = L_{\text{N}}$.

In the presence of an external electric field $\mathbf{E}$, a further contribution to the free-energy must be added. To the lowest order it reads

$$\mathcal{F}_{\text{electric}} = \int f_{\text{E}}(E,S,\psi) \, \mathrm{d}V \ , \tag{3a}$$

$$f_{\text{E}}(E,S,\psi) = \mu E^2 S + \frac{1}{2} \mu' E^2 \psi^2 \ , \tag{3b}$$

where the first term in the right hand side of equation (3b) describes the dielectric coupling and the second one the so-called smectic electrostriction. For strong smectic-nematic coupling γ, which is the case that we consider, the smectic electrostriction is negligible [10]. Therefore, we put $\mu' = 0$. The coupling constant μ is proportional to the molecular dielectric anisotropy $\epsilon_{\text{a}0}$, $\mu = -\epsilon_{\text{a}0}/12\pi$. In the following we shall analyze the case of positive molecular dielectric anisotropy $\epsilon_{\text{a}0} > 0$, which leads to an enhancement of the nematic ordering. With our choice of parameters, the application of the electric field induces a *nonspontaneous* nematic phase [9].

Near a solid surface, for steric reasons, the smectic ordering might be enhanced [16]. Let us then consider a semi-infinite sample filling the half space $z \geq 0$. The presence of the solid boundary at $z = 0$ introduces, at the lowest order, the surface contribution [15]

$$\mathcal{F}_{\text{surface}} = -w \int \psi(z=0) \, \mathrm{d}x \, \mathrm{d}y \ , \tag{4}$$

with $w > 0$. Let us note that terms linear in ψ are forbidden in the bulk as the choice of the origin of the reference frame is arbitrary. This is no more true when a boundary is present that fixes the position of the smectic layers.

The free-energy of the entire system reads

$$\mathcal{F} = \mathcal{F}_{\text{bulk}} + \mathcal{F}_{\text{electric}} + \mathcal{F}_{\text{surface}} \ . \tag{5}$$

Minimization of the latter

$$\delta\mathcal{F} = 0 \Rightarrow \delta \int_0^\infty \Big[f_{\text{N}}(T,S) + f_{\text{A}}(T,\psi) + f_{\text{AN}}(S,\psi) + f_{\text{E}}(E,S,\psi) + \frac{1}{2} L_{\text{N}} \left(\frac{\mathrm{d}S}{\mathrm{d}z}\right)^2 + \frac{1}{2} L_{\text{A}} \left(\frac{\mathrm{d}\psi}{\mathrm{d}z}\right)^2 \Big] \, \mathrm{d}z - w \delta\psi(z=0) = 0 \ , \tag{6}$$

leads to the Euler-Lagrange equations defining the equilibrium order parameters profiles $S(z)$ and $\psi(z)$

$$L_{\rm N}\frac{{\rm d}^2S}{{\rm d}z^2} = \frac{\partial f_{\rm N}}{\partial S} + \frac{\partial f_{\rm AN}}{\partial S} + \frac{\partial f_{\rm E}}{\partial S}\,, \tag{7a}$$

$$L_{\rm A}\frac{{\rm d}^2\psi}{{\rm d}z^2} = \frac{\partial f_{\rm A}}{\partial \psi} + \frac{\partial f_{\rm AN}}{\partial \psi}\,, \tag{7b}$$

with the boundary conditions

$$\left.\frac{{\rm d}S}{{\rm d}z}\right|_{z=0} = \left.\frac{{\rm d}S}{{\rm d}z}\right|_{z=\infty} = \left.\frac{{\rm d}\psi}{{\rm d}z}\right|_{z=\infty} = 0,\ L_{\rm A}\left.\frac{{\rm d}\psi}{{\rm d}z}\right|_{z=0} = -w. \tag{8}$$

The Euler-Lagrange equations can be put into a more convenient form by introducing the following rescaled quantities

$$\begin{aligned}
t &= \frac{T-T_{\rm N}^*}{T_{\rm NI}-T_{\rm N}^*}\,, \quad t_{\rm A}^* = \frac{T_{\rm A}^*-T_{\rm N}^*}{T_{\rm NI}-T_{\rm N}^*}\,, \quad \gamma_{\rm N} = \frac{c_{\rm N}}{b_{\rm N}}\,,\\
\alpha &= \frac{a_{\rm A}}{a_{\rm N}}\,, \quad \gamma_{\rm A} = \frac{c_{\rm A}}{a_{\rm N}(T_{\rm NI}-T_{\rm N}^*)}\\
\Gamma &= \frac{\gamma}{a_{\rm N}(T_{\rm NI}-T_{\rm N}^*)}\,, \quad \Lambda = \frac{\lambda}{a_{\rm N}(T_{\rm NI}-T_{\rm N}^*)}\,,\\
e &= \sqrt{\frac{-\mu}{a_{\rm N}(T_{\rm NI}-T_{\rm N}^*)}}\,E\,,\\
\xi &= \sqrt{\frac{L_{\rm N}}{2a_{\rm N}(T_{\rm NI}-T_{\rm N}^*)}}\,,\\
\zeta &= z/\xi\,, \quad h = \frac{\xi}{L_{\rm A}}w\,, \quad L = \frac{L_{\rm A}}{L_{\rm N}}\,,
\end{aligned} \tag{9}$$

where

$$T_{\rm NI} = T_{\rm N}^* + \frac{2b_{\rm N}^2}{9a_{\rm N}c_{\rm N}} \tag{10}$$

is the nematic–isotropic transition temperature of the uncoupled system. Substituting (9) into (7) and (8) gives

$$\begin{aligned}
\frac{{\rm d}^2S}{{\rm d}\zeta^2} &= F(S,\psi)\\
&= \frac{1}{2}\left[tS + \frac{9}{2}\gamma_{\rm N}S^2 + \frac{9}{2}\gamma_{\rm N}^2S^3 + \Gamma\psi^2 + \Lambda S\psi^2 - e^2\right],
\end{aligned} \tag{11a}$$

$$\begin{aligned}
\frac{{\rm d}^2\psi}{{\rm d}\zeta^2} &= G(S,\psi)\\
&= \frac{1}{2L}\left[\alpha(t-t_{\rm A}^*)\psi + \gamma_{\rm A}\psi^3 + 2\Gamma S\psi + \Lambda S^2\psi\right],
\end{aligned} \tag{11b}$$

$$\left.\frac{{\rm d}S}{{\rm d}\zeta}\right|_{\zeta=0} = \left.\frac{{\rm d}S}{{\rm d}\zeta}\right|_{\zeta=\infty} = \left.\frac{{\rm d}\psi}{{\rm d}\zeta}\right|_{\zeta=\infty} = 0,\ \left.\frac{{\rm d}\psi}{{\rm d}\zeta}\right|_{z=0} = -h. \tag{11c}$$

In order to determine the order parameters profiles $S(\zeta)$ and $\psi(\zeta)$, the boundary value problem (11) has to be solved numerically. It is then convenient to analyze first the asymptotic behavior of $S(\zeta)$ and $\psi(\zeta)$, as they approach the bulk values $S_{\rm B}$ and $\psi_{\rm B}$. The latter are the order parameters which minimize the bulk free-energy $\mathcal{F}_{\rm bulk}$. By setting $\delta S = S - S_{\rm B}$, $\delta\psi = \psi - \psi_{\rm B}$ and linearizing equations (11a, 11b), one obtains

$$\frac{{\rm d}^2}{{\rm d}\zeta^2}\begin{pmatrix}\delta S\\ \delta\psi\end{pmatrix} = A\begin{pmatrix}\delta S\\ \delta\psi\end{pmatrix}\,, \tag{12}$$

where the constant matrix A reads

$$A = \begin{pmatrix}\left.\frac{\partial F}{\partial S}\right|_{(S_{\rm B},\psi_{\rm B})} & \left.\frac{\partial F}{\partial \psi}\right|_{(S_{\rm B},\psi_{\rm B})}\\ \left.\frac{\partial G}{\partial S}\right|_{(S_{\rm B},\psi_{\rm B})} & \left.\frac{\partial G}{\partial \psi}\right|_{(S_{\rm B},\psi_{\rm B})}\end{pmatrix}\,. \tag{13}$$

Diagonalizing the matrix A and keeping only the decaying solutions, one arrives at

$$\begin{pmatrix}\delta S(\zeta)\\ \delta\psi(\zeta)\end{pmatrix} = Z\begin{pmatrix}\exp(-\sqrt{D_1}\zeta) & 0\\ 0 & \exp(-\sqrt{D_2}\zeta)\end{pmatrix}Z^{-1}\begin{pmatrix}a\\ b\end{pmatrix}\,, \tag{14}$$

where Z contains the eigenvectors of the matrix A arranged in columns, D_1 and D_2 are the corresponding eigenvalues, and a, b are integration constants. The asymptotic boundary conditions are then obtained by differentiating the equation above (14)

$$\frac{\rm d}{{\rm d}\zeta}\begin{pmatrix}\delta S(\zeta)\\ \delta\psi(\zeta)\end{pmatrix} = -Z\begin{pmatrix}\sqrt{D_1} & 0\\ 0 & \sqrt{D_2}\end{pmatrix}Z^{-1}\begin{pmatrix}\delta S(\zeta)\\ \delta\psi(\zeta)\end{pmatrix}\,. \tag{15}$$

3 Analysis

The Euler-Lagrange equations (11a, 11b) were solved numerically using a standard finite difference scheme with deferred correction and Newton iteration [17]. We used the exact boundary conditions at $\zeta = 0$, while those at infinity were substituted by the asymptotic ones (15) evaluated at sufficiently large ζ. When multiple solutions were present, the one corresponding to the lowest total free-energy (5) was selected.

Let us focus our attention on the behavior of the surface order parameters, namely, $S_0 \equiv S(\zeta = 0)$ and $\psi_0 \equiv \psi(\zeta = 0)$. The corresponding phase diagrams are presented in the plane of the reduced field e and temperature t. They were determined by analyzing the behavior of S_0 and ψ_0 for fixed field e as a function of the temperature t, or equivalently, for fixed temperature t as a function of the field e. The material parameters were kept fixed, while the effect of the surface coupling constant h was investigated, as displayed in Figures 1–3.

When no surface coupling is present ($h = 0$), the order parameters profiles are flat: the surface order parameters S_0 and ψ_0 *coincide* with the bulk ones. The corresponding phase diagram is shown in Figure 1. If there is no electric field e, a direct isotropic to smectic-A transition occurs on cooling. However, for infinitesimally small field, the isotropic phase is replaced by a paranematic (pN) one. The latter is characterized by $S > 0$ and $\psi = 0$.

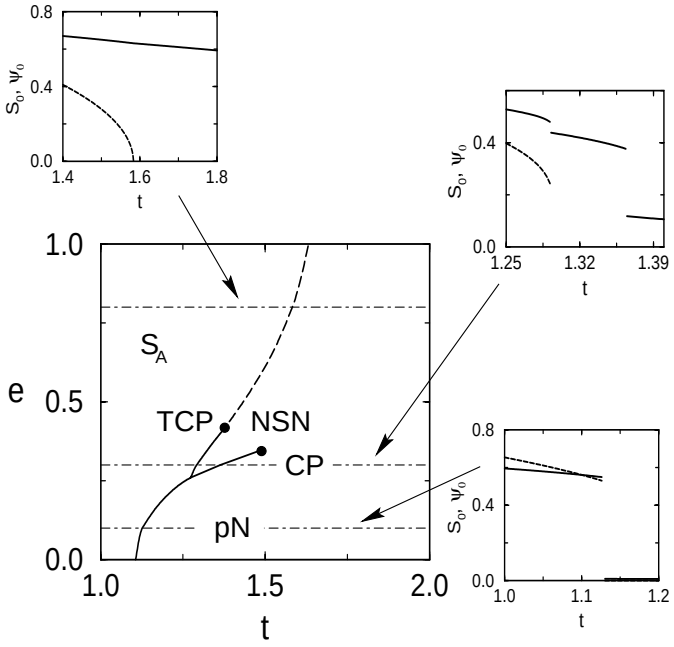

Fig. 1. Surface phase diagram in the (e, t) plane for $h = 0$. The solid lines refer to first-order transitions, the dashed line to a second-order one. The outer graphs display the behavior of S_0 (solid line) and ψ_0 (dashed line) as a function of the reduced temperature t for the three values of the reduced electric field $e = 0.1$, $e = 0.3$, $e = 0.8$ indicated by the dotted-dashed lines in the phase diagram.

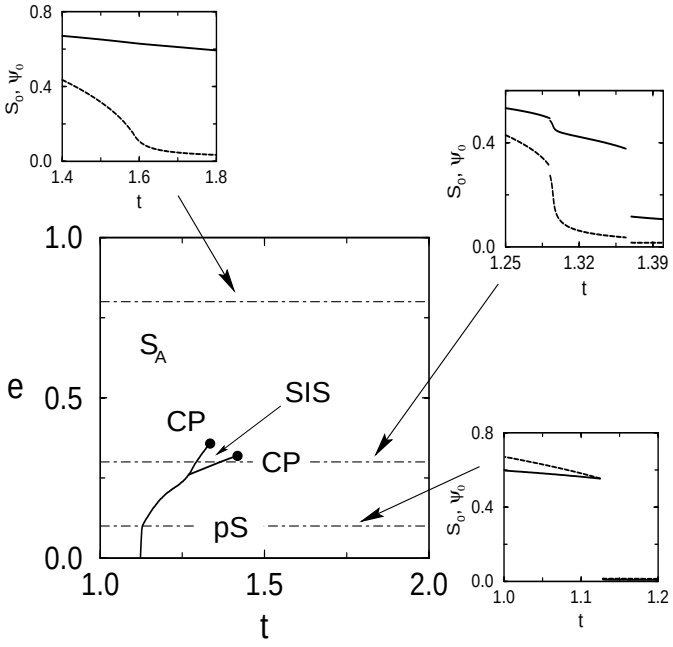

Fig. 2. Same as Figure 1 but for $h = 0.01$.

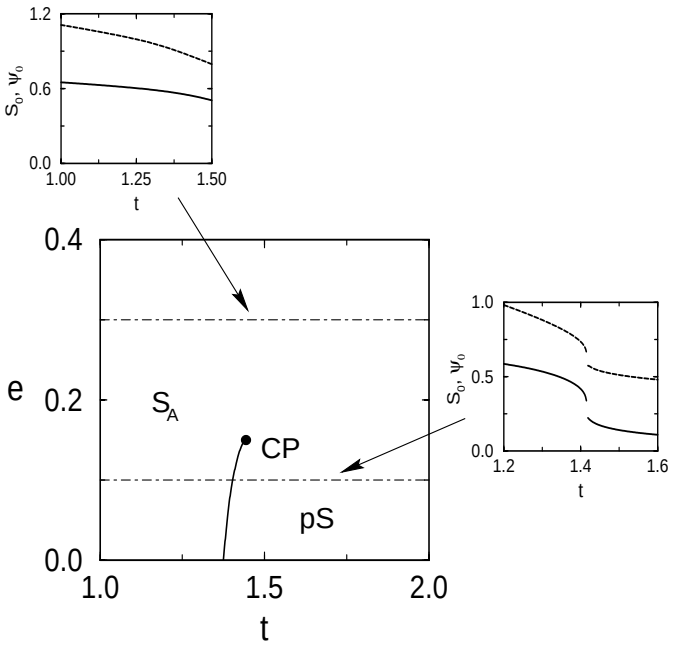

Fig. 3. Same as Figure 1 but for $h = 0.35$. The outer graphs correspond to $e = 0.1$ and $e = 0.3$.

As the electric field is increased, the $\mathrm{pN} - \mathrm{S_A}$ transition temperature shifts toward higher values. Above a suitable value of the field, a nonspontaneous nematic (NSN) phase appears between the paranematic and the smectic ones, separated from them by first-order transition lines. The one delimiting the $\mathrm{pN} - \mathrm{NSN}$ phases terminates at the critical point CP, while the other one transforms into a second-order transition line above the tricritical point TCP. This phase diagram summarizes the results presented in [9].

The case of small surface coupling h is analyzed in Figure 2. The pN and the NSN bulk phases are replaced by a parasmectic (pS) and a surface-induced-smectic (SIS) phase, respectively. They are both characterized by $S > 0$ and $\psi > 0$. The bulk tricritical point TCP transforms now into a critical point CP as the smectic $\mathrm{S_A}$ and SIS phases have the same symmetry.

Further increasing of the surface coupling leads to the behavior displayed in Figure 3. Only smectic and parasmectic phases are present, separated by a first-order transition line terminating at a critical point. Finally, above a threshold value $h \geq h_t = 0.39$, the whole (e, t) plane is occupied by the smectic $\mathrm{S_A}$ phase.

One should also notice that the transition temperatures at the surface are generally shifted with respect to the bulk ones. This is illustrated in Figure 4 for the case of the pS to $\mathrm{S_A}$ transition in the absence of electric field. For low coupling h, the surface transition temperature coincides with the bulk one. Above a certain threshold, that for the case shown in Figure 4 corresponds to $h = 0.235$, the surface transition temperature begins to shift toward higher values, while at the same time the jumps in the order parameters decrease. The derivative of the smectic surface order parameter ψ_0 develops a discontinuity at the bulk transition temperature. No such feature is apparent in S_0, which is not directly coupled to the surface.

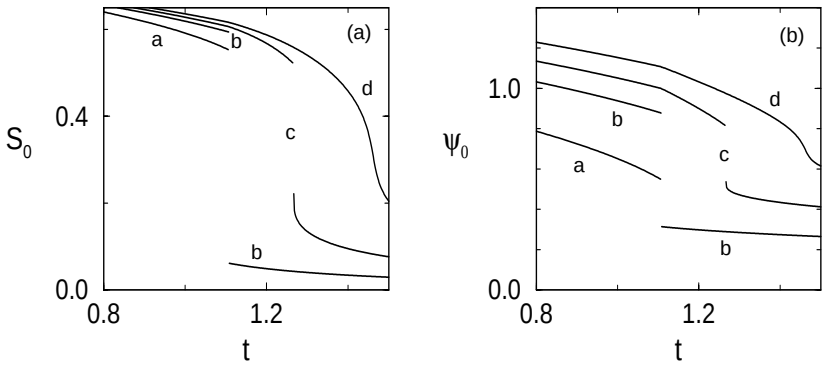

Fig. 4. Surface order parameters S_0 (a) and ψ_0 (b) as a function of the reduced temperature t for $e = 0$. The surface coupling constant h is equal to $h = 0$ (curves a), $h = 0.2$ (curves b), $h = 0.3$ (curves c), and $h = 0.4$ (curves d).

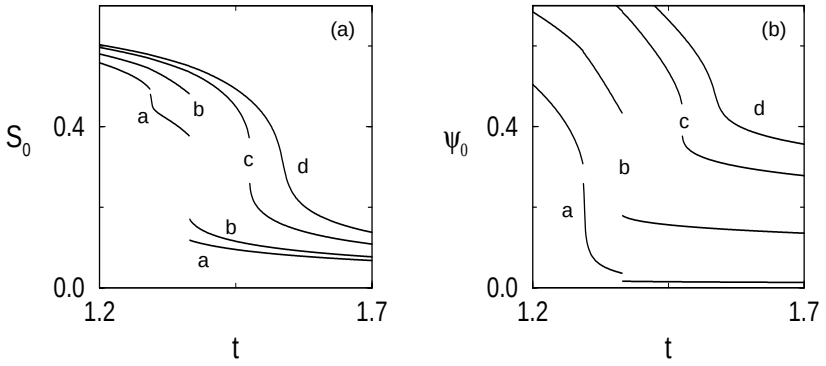

Fig. 5. Same as Figure 4 but for $e = 0.3$. Here the surface coupling constant h is equal to $h = 0.01$ (curves a), $h = 0.1$ (curves b), $h = 0.2$ (curves c), and $h = 0.25$ (curves d).

Above a critical value of h, equal to $h = 0.39$ for the case considered here, the transition disappears. A similar behavior was found in the boundary-layer transition in nematic liquid crystals [18]. Figure 5 shows the effect of the surface coupling when an external electric field is present, such that a nonspontaneous nematic appears in the bulk. As h is increased, the S_A to SIS surface transition progressively disappears, while remaining at the same temperature as the corresponding S_A to NSN bulk transition. At the same time, the SIS to pS surface transition is not shifted with respect to the corresponding NSN to pN bulk one. However, as the surface coupling is further increased, the SIS to pS surface transition begins to shift as before. Correspondingly, it becomes less pronounced, until it disappears at the critical point.

4 Conclusions

The phase behavior of liquid-crystal systems is strongly affected by the proximity of boundaries. In the past, various theoretical [18–21] and experimental [22] investigations have been aimed at understanding the influence of the nematic-surface interactions on the local ordering at interfaces. As it has been shown, the presence of a boundary can lead to a variety of interesting phenomena as, *e.g.*, temperature shifts of the phase transitions and different transitions between surface-oriented states. No such thorough analysis has been performed in the case of smectogenic materials, even if, as suggested by experiments [12,9], in this situation the presence of a surface can strongly influence the thermodynamic behavior of the system.

In this paper, by means of a Landau-de Gennes approach, we have analyzed the surface phase diagram of a semi-infinite liquid crystalline sample displaying a direct isotropic to smectic-A transition in the bulk. The combined effect of an external electric field and of an ordering solid surface has been analyzed. The Euler-Lagrange equations describing the equilibrium order parameters profiles have been solved exactly using a standard finite difference scheme with deferred correction and Newton iteration [17]. Two new surface phases, namely a parasmectic and a surface-induced smectic phase have been described. The existence of two surface critical points has been predicted, one corresponding to the bulk critical point terminating the paranematic to nonspontaneous nematic transition, and the other one replacing the bulk tricritical point of the nematic to smectic-A transition. Shifts in the surface transition temperatures have been predicted, similarly to the case of nematogenic materials. An experimental verification of these results is still lacking and could be performed by means of surface X-ray scattering measurements.

To conclude, we note that our continuum model applies only when the correlation length ξ is sufficiently large with respect to the thickness of the smectic layers. This is indeed the case of some smectogenic materials that have been analyzed in the past, without however investigating the effect of an external electric field [11]. Moreover, for the sake of simplicity, in this analysis we have not taken into account the possibility of a direct coupling of the nematic order parameter S with the surface. As it has been

pointed out in reference [16], for small ξ values such a coupling may lead to a sharp smectic interface occurring at a finite distance from the solid interface. We finally note that the case of a sample having a finite thickness comparable with the smectic layers' distance, that we have not considered here, is much more complex to tackle, as frustration effects are expected to occur [15].

We thank G. Barbero for fruitful discussions. M.Ż. gratefully acknowledges MURST for financial support in the framework of the collaboration between Politecnico di Torino and Raman Research Institute of Bangalore.

References

1. J. Prost, P.G. de Gennes, *The Physics of Liquid Crystals* (Clarendon Press, Oxford, 1993).
2. J. Hanus, Phys. Rev. **178**, 420 (1969).
3. P.J. Wojtowicz, P. Sheng, Phys. Lett. **48A**, 235 (1974).
4. R.M. Hornreich, Phys. Lett. **109A**, 232 (1985).
5. I. Lelidis, M. Nobili, G. Durand, Phys. Rev. E **48**, 3818 (1993).
6. I. Lelidis, G. Durand, Phys. Rev. E **48**, 3822 (1993).
7. H. Hama, J. Phys. Soc. Jpn **54**, 2204 (1985).
8. C. Rosenblatt, J. Phys. Lett. France **42**, L9 (1981); Phys. Lett. A **83**, 221 (1981).
9. I. Lelidis, G. Durand, Phys. Rev. Lett. **73**, 672 (1994).
10. I. Lelidis, G. Durand, J. Phys. II France **6**, 1359 (1996).
11. J. Als-Nielsen, F. Christensen, P.S. Pershan, Phys. Rev. Lett. **48**, 1107 (1982).
12. B.M. Ocko, Phys. Rev. Lett. **64**, 2160 (1990).
13. J. Stelzer, *Molekulardynamische Studien von Oberflächeneffekten nematischer Flüssigkristalle* (Ph. D. Thesis, Institut für Theoretische und Angewandte Physik, Universität Stuttgart, 1995).
14. J. Stelzer, P. Galatola, G. Barbero, L. Longa, Phys. Rev. E **55**, 477 (1997).
15. P.G. de Gennes, Langmuir **6**, 1448 (1990).
16. B.M. Ocko, A. Braslau, P.S. Pershan, J. Als-Nielsen, M. Deutsch, Phys. Rev. Lett. **57**, 94 (1986).
17. U. Ascher, R.M.M. Mattheij, R.D. Russell, *Numerical Solution of Boundary Value Problems for Ordinary Differential Equations* (Prentice Hall, Englewood Cliffs, NJ, 1988).
18. Ping Sheng, Phys. Rev. Lett **37**, 1059 (1976); Phys. Rev. A **26**, 1610 (1982).
19. Z. Pawlowska, T.J. Sluckin, G.F. Kventsel, Phys. Rev. A **38**, 5342 (1988); J.V. Selinger, D.R. Nelson, Phys. Rev. A **37**, 1736 (1988).
20. R. Lipowsky, Phys. Rev. Lett. **49**, 1575 (1982); R. Lipowsky, W. Speth, Phys. Rev. B **28**, 3983 (1983).
21. G. Barbero, E. Miraldi, A. Stepanescu, J. Appl. Phys. **68**, 2063 (1990).
22. K. Myano, Phys. Rev. Lett. **43**, 51 (1979).